

## Size-Dependent Pressure-Induced Amorphization in Nanoscale TiO<sub>2</sub>

Varghese Swamy,<sup>1,\*</sup> Alexei Kuznetsov,<sup>2</sup> Leonid S. Dubrovinsky,<sup>2</sup> Paul F. McMillan,<sup>3,†</sup> Vitali B. Prakapenka,<sup>4</sup> Guoyin Shen,<sup>4</sup> and Barry C. Muddle<sup>1</sup>

<sup>1</sup>Department of Materials Engineering, Monash University, P.O. Box 69M, Victoria 3800, Australia

<sup>2</sup>Bayerisches Geoinstitut, Universität Bayreuth, Bayreuth D-95440, Germany

<sup>3</sup>Department of Chemistry and Materials Chemistry Centre, University College London, 20 Gordon Street, London WC1H 0AJ, United Kingdom

<sup>4</sup>Consortium for Advanced Radiation Sources, University of Chicago, Chicago, Illinois 60637, USA

(Received 16 January 2006; published 5 April 2006)

We investigated the size-dependent high-pressure phase transition behavior of nanocrystalline anatase TiO<sub>2</sub> with synchrotron x-ray diffraction and Raman spectroscopy to 45 GPa at ambient temperature. Pressure-induced amorphization results in a high-density amorphous (HDA) form when the starting crystallite size is <10 nm. The HDA-TiO<sub>2</sub> transforms to a low-density amorphous form at lower pressures. Harnessing the nanometer length scale thus provides a new window for experimental investigation of amorphization in poor glass formers and a synthesis route for new amorphous materials.

DOI: 10.1103/PhysRevLett.96.135702

PACS numbers: 64.70.Nd, 61.43.Er, 61.82.Rx, 62.50.+p

Pressure-induced amorphization (PIA) has been observed for many classes of materials [1,2]. The phenomenon involves metastable transformation of crystalline materials into amorphous solids by application of pressure ( $P$ ) at a temperature ( $T$ ) that is sufficiently low to preclude nucleation and growth of stable crystalline phases. It is a kinetically controlled event correlated with a frustrated attempt by the crystal to reach its stable packing at high density. Mechanical instabilities developed in the metastably compressed crystal can give rise to spinodal behavior, and PIA can also take on a thermodynamic character, such as the glass transition approaching the Kauzmann limit [3]. PIA has been mostly described among tetrahedrally coordinated solids (e.g., SiO<sub>2</sub>, H<sub>2</sub>O, and Si) [1,2]. In the cases of H<sub>2</sub>O and Si, PIA results in new high-density amorphous (HDA) forms that can either be recovered metastably to ambient  $P$  or transformed to low-density amorphous (LDA) structures during decompression [1,4]. The HDA-LDA polyamorphism is usually linked to an underlying density-driven liquid-liquid phase transition [4]. In this Letter, we report PIA leading to HDA and LDA forms among nanocrystalline samples of the octahedrally coordinated TiO<sub>2</sub>.

Bulk TiO<sub>2</sub> is a poor glass former. Amorphous TiO<sub>2</sub> ( $a$ -TiO<sub>2</sub>), an important technological material, is usually obtained via sol-gel techniques.  $a$ -TiO<sub>2</sub> could be obtained by PIA, but the application of pressure (compression, decompression, or shock-wave) is not known to amorphize bulk TiO<sub>2</sub> crystals. However, surface vs bulk free energy contributions within nanocrystalline materials (TiO<sub>2</sub>, ZrO<sub>2</sub>, Al<sub>2</sub>O<sub>3</sub>, etc.) are known to result in reversals of normal stability relations among bulk phases [5,6], and may stabilize the amorphous form at high pressures. Recently, it was reported that pressure-induced phase transitions in nanocrystalline ( $nc$ ) anatase (tetragonal space group  $I4_1/amd$ , designated  $t$ -TiO<sub>2</sub>) are particle size de-

pendent [7] (Fig. 1). Crystallites with sizes >50 nm transform to thermodynamically stable TiO<sub>2</sub>-II ( $\alpha$ -PbO<sub>2</sub> structure,  $Pbcn$ ;  $o$ -TiO<sub>2</sub>) at  $P > 5$  GPa. Twelve to 50 nm  $nc$ - $t$ -TiO<sub>2</sub> particles transform to monoclinic baddeleyite-structured TiO<sub>2</sub> ( $P2_1/c$ ;  $m$ -TiO<sub>2</sub>) at 12–20 GPa. Materials obtained by high- $P$  treatment of smaller (< 10 nm) nanocrystals appeared to be amorphous [7]. Here, we examined the  $P$ -dependent changes in  $nc$ - $t$ -TiO<sub>2</sub> with crystallite

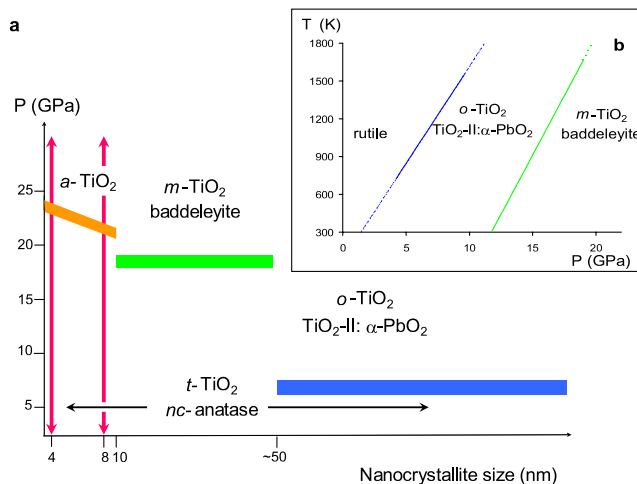


FIG. 1 (color online). (a) Size-dependent pressure stability of  $nc$ - $t$ -TiO<sub>2</sub> (modified after Ref. [7]). The average transition pressures of the three phase transition regimes are shown. Nanocrystals of size <10 nm undergo PIA and remain amorphous ( $a$ -TiO<sub>2</sub>) upon further compression and decompression. Approximately 12–50 nm crystallites transform to  $m$ -TiO<sub>2</sub> upon compression, which then transforms to  $o$ -TiO<sub>2</sub> on decompression. Coarser crystallites transform directly to  $o$ -TiO<sub>2</sub>. The compression-decompression paths of the two samples of this study are indicated. (b) Known stable  $P$ - $T$  relations [9,19–21] in the bulk TiO<sub>2</sub> system.

sizes  $<10$  nm using angle-dispersive synchrotron x-ray diffraction (XRD) and Raman spectroscopy in diamond-anvil cells (DACs) at ambient  $T$  and  $P$  up to 45 GPa [8]. Starting materials included  $nc$ -anatase with average sizes  $4 \pm 1$  nm (sample A) or  $8 \pm 2$  nm (sample B) (Fig. 1).

Samples A and B exhibit similar behavior during compression to 45 GPa and subsequent decompression to ambient  $P$ . The  $t$ -TiO<sub>2</sub> structure is retained metastably to  $P = 20$ –24 GPa during compression, with PIA occurring beyond this pressure range (Fig. 2). During a typical compression-decompression cycle, the  $nc$ -anatase XRD peaks broadened and weakened with increasing  $P$  to  $\sim 20$  GPa; spectra obtained following decompression from 45 GPa showed very broad features typical of  $a$ -TiO<sub>2</sub>. The broad features in the high- $P$  ( $>20$  GPa) XRD spectra could not be correlated with the diffraction patterns of any known TiO<sub>2</sub> phases stable in this pressure range [e.g.,  $m$ -TiO<sub>2</sub> [9], OI ( $Pbca$ ) [10], or OII ( $Pnma$ ) [11]]. Weak peaks occurring in the spectrum of sample B on decompression to 0 GPa may suggest increased ordering in the  $a$ -TiO<sub>2</sub> (Fig. 2). Again, the broad bands observed for sample A resemble the diffraction peaks of  $o$ -TiO<sub>2</sub>. However, transmission electron microscopy and electron diffraction studies do not indicate the presence of any crystalline material [Fig. 2(d)]. We suggest that the

$a$ -TiO<sub>2</sub> recovered to ambient  $P$  is noncrystalline but has a structural relationship to  $o$ -TiO<sub>2</sub>. The  $a$ -TiO<sub>2</sub> formed by PIA at high- $P$  is likely to be structurally related to  $m$ -TiO<sub>2</sub> (Figs. 3 and 4). In that case, the data indicate a polyamorphic transformation occurring during decompression of  $a$ -TiO<sub>2</sub> between an HDA form produced by PIA and an LDA polyamorph that is recovered at ambient  $P$ . This is similar behavior to H<sub>2</sub>O and  $a$ -Si produced by PIA of nanocrystalline porous-Si materials [12,13]. Interestingly, the high- and low- $P$  XRD spectra of  $a$ -TiO<sub>2</sub> are similar to those obtained at similar pressures from a chemically synthesized sample during a decompression run from similar peak pressure (Ref. [8], Fig. S1). The two amorphous structures show distinct pressure dependencies as seen in the pressure evolution of their major broad feature in the XRD spectra (Ref. [8], Fig. S4).

In order to characterize the pressure-dependent  $a$ -TiO<sub>2</sub> structures, we obtained Raman spectra during compression-decompression cycles. Raman spectroscopy is highly sensitive to phase changes occurring in  $nc$ -TiO<sub>2</sub> [7], and it provides a detailed structural probe of local coordination environments [12]. In Fig. 3 we present Raman spectra of  $nc$ - $t$ -TiO<sub>2</sub> and  $a$ -TiO<sub>2</sub> materials measured during compression and decompression of sample A. (Additional data are presented in Ref. [8], Figs. S2 and S3.)

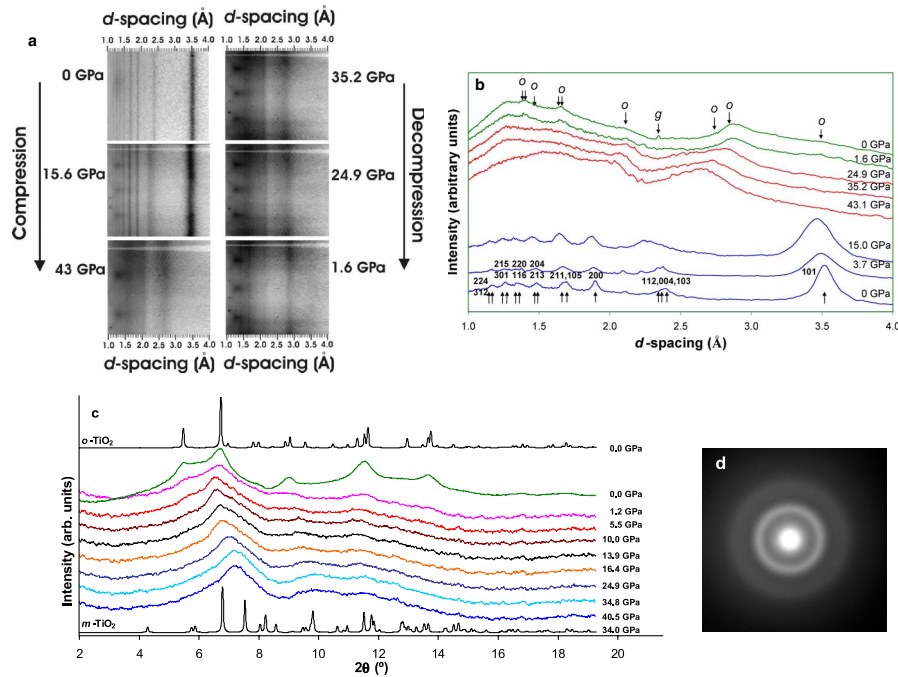


FIG. 2 (color online). Synchrotron XRD data obtained during compression and decompression of  $nc$ - $t$ -TiO<sub>2</sub> particles. (a) PIA takes place in sample B (8 nm particles) at  $\sim 20$  GPa (left column). The amorphous phase is recovered to ambient conditions, but subtle changes in the XRD pattern, including increased ordering at low pressures, are observed upon decompression (right column). (b) Integrated XRD data of sample B during compression or decompression runs. Anatase ( $t$ -TiO<sub>2</sub>) reflections are indicated by “up” arrow; arrows labeled “ $o$ ” and “ $g$ ” represent  $o$ -TiO<sub>2</sub> and Au diffraction positions at 0 GPa. (c) Integrated XRD data of sample A (4 nm) obtained during decompression. Calculated XRD spectra (for wavelength  $\lambda = 0.3344$  Å) of  $o$ -TiO<sub>2</sub> and  $m$ -TiO<sub>2</sub> are given for comparison. The 0 GPa (outside the DAC) spectrum of pressure-amorphized sample A exhibits diffuse scattering background characteristic of a highly disordered material, with perhaps structural similarity to  $o$ -TiO<sub>2</sub>. Electron diffraction (d), however, confirms the amorphous nature of the material at a length scale of that of a crystalline unit cell ( $\sim 1$  nm).

The strong  $E_g$  Raman mode of *nc*-anatase at  $\sim 144$   $\text{cm}^{-1}$  is observable to 20–24 GPa. Raman spectra obtained above this pressure exhibit a broad density-of-states function with broad weak maxima near 225–290  $\text{cm}^{-1}$  and 495–540  $\text{cm}^{-1}$  [Fig. 3(a)]. During decompression, new broad features began to emerge at high (550–650  $\text{cm}^{-1}$ ) and low wave numbers (100–300  $\text{cm}^{-1}$ ) below  $P = 15$ –16 GPa for both samples, indicating the presence of a LDA polyamorph. The new peaks grew and redshifted with decreasing pressure, evolving into a distinct LDA spectrum below  $P \sim 10$  GPa [Fig. 3(b)]. The ambient  $P$  spectra from recovered material are different from those of sol-gel produced *a*-TiO<sub>2</sub> that has been shown to be structurally related to brookite or anatase [14]. Upon recompression, the LDA-TiO<sub>2</sub> spectrum transformed back into that of the HDA polyamorph above  $P \sim 15$  GPa, suggesting the possibility of a reversible HDA-LDA polyamorphic transition such as that observed for *a*-H<sub>2</sub>O and *a*-Si [12,13] (Ref. [8], Fig. S3).

Comparison of the XRD and Raman spectra obtained at high and low pressures from *a*-TiO<sub>2</sub> with that of various crystalline phases reveals that the HDA and LDA forms might be structurally related to *m*-TiO<sub>2</sub> and *o*-TiO<sub>2</sub>, respectively (Fig. 4). The *o*-TiO<sub>2</sub> structure consists of a planar arrangement of distorted TiO<sub>6</sub> octahedra sharing

edges to form zigzag chains along the *c* direction that are linked through octahedral corners [15]. *m*-TiO<sub>2</sub> has a distorted fluorite structure in which each Ti atom is coordinated to 7 oxygens [9]. The *o*-TiO<sub>2</sub>-*m*-TiO<sub>2</sub> phase transition in the bulk material at ambient  $T$  and  $P \sim 12$  GPa [9] involves a 6 to 7 Ti-O coordination change, accompanied by a volume reduction of  $\sim 9\%$ . The structural similarities between low- and high- $P$  crystalline phases and the corresponding LDA/HDA polyamorphs suggest similar density differences [16]. Based on these observations, we suggest that *a*-TiO<sub>2</sub> produced via PIA from nanoscale materials exhibits  $P$ -dependent structural variations with an *o*-TiO<sub>2</sub>-type component dominating at low pressures ( $< 16$  GPa) and an *m*-TiO<sub>2</sub>-type component stabilized at higher pressures, and that a  $P$ -induced LDA-HDA transition may occur between the two polyamorphic forms. Future experiments are needed to determine the exact nature of the transition.

PIA leading to the HDA and LDA forms in *nc-t*-TiO<sub>2</sub> described above is similar to that reported for ice (H<sub>2</sub>O) [13] and for porous Si [12]. The telltale signs of a system with potential for PIA and a density-driven polyamorphic transition include melting with a negative Clapeyron ( $-dT_m/dP$ ) slope or the appearance of maxima in the melting curve [16] and negative thermal expansion of low-pressure crystals observed among flexible framework structures [17]. A thermodynamic explanation of PIA involves interception along the compression or decompression path of the metastable extension of the melting curve (with negative slope or a maximum); this approach has been successfully applied to understand the phenomena in ice [13], silica [18], Si [12], and other materials [16]. We cannot yet test this proposition for TiO<sub>2</sub> because the available high- $P$ ,  $T$  phase relations [9,19–21] do not include melting curve determinations, and stable vs metastable

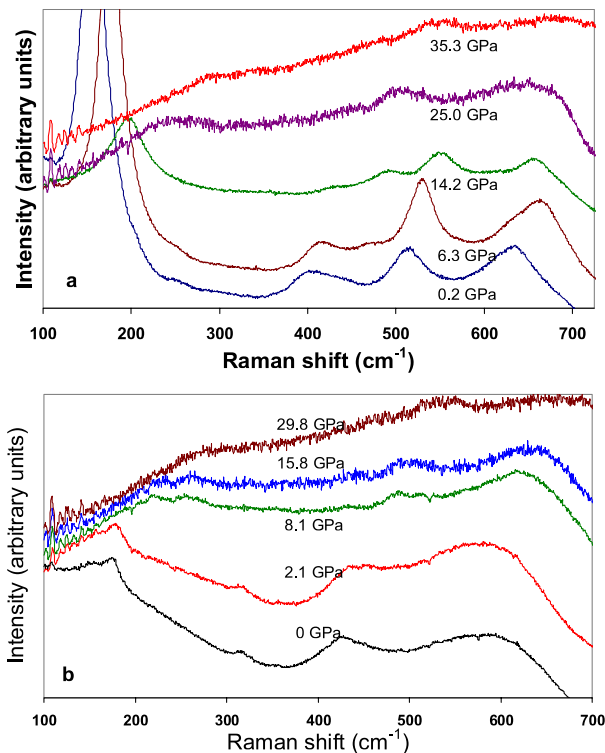


FIG. 3 (color online). Raman spectra of sample A measured during compression and decompression. (a) Compression. The bottom three spectra show the pressure evolution of anatase (*nc-t*-TiO<sub>2</sub>) Raman modes. PIA occurs at  $P > 20$  GPa. (b) During decompression, spectral changes indicate structural modification within the *a*-TiO<sub>2</sub> materials produced via PIA.

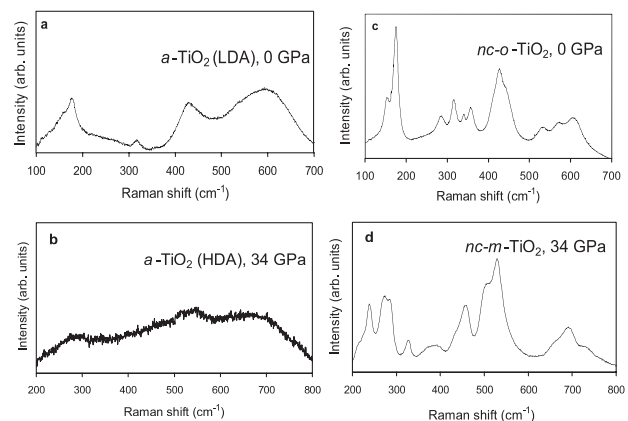


FIG. 4. Comparison of low- and high- $P$  Raman spectra of *a*-TiO<sub>2</sub> with those of crystalline polymorphs. (a) Raman spectrum of *a*-TiO<sub>2</sub>/LDA (sample B) decompressed to 0 GPa. (b) Raman spectrum of *a*-TiO<sub>2</sub>/HDA (sample A) at 34 GPa. (c) Raman spectrum of *nc-o*-TiO<sub>2</sub> ( $\sim 11$  nm) at 0 GPa. (d) Raman spectrum of *nc-m*-TiO<sub>2</sub> ( $\sim 30$  nm) obtained at 34 GPa [26].

transformations for TiO<sub>2</sub> polymorphs, including melting, are strongly modified by surface energy contributions within nanocrystalline materials [5,22–24]. Our results indicate that PIA can occur for nanoparticles among systems that are poor glass formers, and that this process could yield useful amorphous ceramics and nanocomposites.

Our study represents a recognition and demonstration of the critical role of finite-particle size determining PIA and possible polyamorphism within poor glass-forming materials. The recently proposed mechanism involving formation of “ferroelastic glass” through the stress-related disintegration into randomly oriented nanoscale domains [25] is not appropriate here, because PIA was observed in sub-10 nm nanocrystals that are unlikely to undergo further fracturing. Coarser TiO<sub>2</sub> nanocrystals were shown to preserve crystallite integrity during pressure cycling across various structural transitions [26]. The observed PIA is size sensitive in that crystallites coarser than  $\sim 10$  nm undergo crystal-crystal transitions, instead of PIA. Finely balanced, size-dependent bulk vs surface energetics are at work here; these also determine the kinetics of stable vs metastable transitions occurring among the crystalline and amorphous materials [5,12,23,24].

Our results presented here and in Ref. [7] allow for a rationalization of the disparate high-pressure data on *nc*-Si [12,27,28] as due to size-dependent phase selectivity: nanocrystals of size less than  $\sim 5$  nm undergo PIA into an HDA form followed by subsequent HDA-LDA transformation during decompression; coarser crystallites undergo stable and metastable crystal-crystal transformations [12]. The thermodynamic/kinetic arguments advanced for Si and H<sub>2</sub>O [12,13] could apply for TiO<sub>2</sub> as well. The PIA phenomenon in Si was linked to the negatively sloping melting curve of the low-*P* phase (diamond-structured Si) that varied as a function of nanocrystallite size [12]. We could envisage a similar picture for TiO<sub>2</sub>, perhaps analogous to melting relations established among substances such as SiO<sub>2</sub> that exhibit PIA and polyamorphism associated with melting curve maxima among tetrahedrally and octahedrally coordinated phases [16,18]. However, that description must await determination of the melting relations for TiO<sub>2</sub> phases at high *P*, *T* for bulk phases as well as nanoparticles.

Our studies demonstrate that PIA occurs within TiO<sub>2</sub> particles (nanocrystalline anatase-structured *t*-TiO<sub>2</sub>) with size below  $\sim 10$  nm in dimension. The PIA-produced *a*-TiO<sub>2</sub> material can be recovered to ambient *P*. Controlled formation of some TiO<sub>2</sub> nanocrystals of metastable phases (e.g., *o*-TiO<sub>2</sub>) within the amorphous matrix could result in new electronic ceramic nanocomposites. The HDA material formed by PIA at high pressure reverts to an LDA-TiO<sub>2</sub> polyamorph during decompression. Although the exact nature of this transition remains unknown, this behavior mimics the high-*P* polyamorphism in *a*-Si and *a*-H<sub>2</sub>O (in *a*-Si the HDA-LDA transition was produced via PIA from nanoparticles). The results show

that PIA of nanocrystalline materials is a useful new method for preparing amorphous solids among the family of materials considered to be “reluctant” glass formers, and also for studying HDA-LDA transformations within a wide range of polyamorphic systems.

We thank Nagayoshi Sata and Yasuo Ohishi (SPring-8, Japan) for the help with the XRD experiment. Ian Grey and Christina Li are thanked for the amorphous TiO<sub>2</sub> material.

---

\*Corresponding author.

Electronic address: Varghese.Swamy@eng.monash.edu.au

<sup>†</sup>Also at Davy-Faraday Research Laboratory, Royal Institution, 21 Albemarle Street, London W1X 4BS, UK.

- [1] E. G. Ponyatovsky and O. I. Barkalov, *Mater. Sci. Rep.* **8**, 147 (1992).
- [2] S. M. Sharma and S. K. Sikka, *Prog. Mater. Sci.* **40**, 1 (1996).
- [3] C. A. Angell, *Science* **267**, 1924 (1995).
- [4] P. F. McMillan, *J. Mater. Chem.* **14**, 1506 (2004).
- [5] A. Navrotsky, *Geochem. Trans.* **4**, 34 (2003).
- [6] J. M. McHale *et al.*, *Science* **277**, 788 (1997).
- [7] V. Swamy *et al.*, *Phys. Rev. B* **71**, 184302 (2005).
- [8] See EPAPS Document No. E-PRLTAO-96-041615 for materials, methods, and additional figures. For more information on EPAPS, see <http://www.aip.org/pubservs/epaps.html>.
- [9] H. Sato *et al.*, *Science* **251**, 786 (1991).
- [10] N. A. Dubrovinskaia *et al.*, *Phys. Rev. Lett.* **87**, 275501 (2001).
- [11] L. S. Dubrovinsky *et al.*, *Nature (London)* **410**, 653 (2001).
- [12] S. K. Deb *et al.*, *Nature (London)* **414**, 528 (2001).
- [13] O. Mishima, L. D. Calvert, and E. Whalley, *Nature (London)* **310**, 393 (1984).
- [14] Q. J. Wang *et al.*, in *Physics and Chemistry of Finite Systems: From Clusters to Crystals*, edited by P. Jena *et al.* (Kluwer, Dordrecht, 1992), Vol. II, pp. 1287–1294.
- [15] B. G. Hyde and S. Andersson, *Inorganic Crystal Structures* (Wiley, New York, 1989).
- [16] P. Richet and P. Gillet, *Eur. J. Mineral.* **9**, 907 (1997).
- [17] C. A. Perottoni and J. A. H. Jornada, *Science* **280**, 886 (1998).
- [18] R. J. Hemley *et al.*, *Nature (London)* **334**, 52 (1988).
- [19] J. S. Olsen, L. Gerward, and J. Z. Jiang, *J. Phys. Chem. Solids* **60**, 229 (1999).
- [20] J. Tang and S. Endo, *J. Am. Ceram. Soc.* **76**, 796 (1993).
- [21] A. C. Withers, E. J. Essene, and Y. Zhang, *Contrib. Mineral. Petrol.* **145**, 199 (2003).
- [22] A. N. Goldstein, C. M. Echer, and A. P. Alivisatos, *Science* **256**, 1425 (1992).
- [23] S. H. Tolbert and A. P. Alivisatos, *Annu. Rev. Phys. Chem.* **46**, 595 (1995).
- [24] S. L. Lai *et al.*, *Phys. Rev. Lett.* **77**, 99 (1996).
- [25] P. Tolédano and D. Machon, *Phys. Rev. B* **71**, 024210 (2005).
- [26] V. Swamy *et al.*, *Solid State Commun.* **134**, 541 (2005).
- [27] S. H. Tolbert *et al.*, *Phys. Rev. Lett.* **76**, 4384 (1996).
- [28] R. A. Senter *et al.*, *Phys. Rev. Lett.* **93**, 175502 (2004).